CENTRAL RESEARCH LIBRARY
DOCUMENT COLLECTION

OAK RIDGE NATIONAL LABORATORY
OPERATED BY
UNION CARBIDE CORPORATION
NUCLEAR DIVISION
POST OFFICE BOX X
OAK RIDGE, TENNESSEE 37830

ORNL-MIT- 81

DATE: May 8, 1969 COPY NO. 29

SUBJECT: A Study of the Dispersion of Gases in Viscous Liquids with Application to Radioactive Krypton and Xenon Disposal, Part I

AUTHOR: M.H. Jorris and L.S. Bowers

Consultants: W.E. Clark and W.F. Schaffer, Jr.

ABSTRACT

The dispersion of argon in polybutene was studied in a continuous flow mixing chamber to define the parameters affecting the dispersion of krypton and xenon in molten glass. Parameters varied were gas flow rate, impeller speed, impeller geometry, and gas inlet position relative to direction of liquid flow. It was found that impeller geometry and gas inlet position had only minor effects. The volumetric percent gas in the foams generated increased linearly as a function of impeller speed, the slope being a function of gas flow rate. Average bubble size decreased with increased impeller speed, but no functionality was determined. Blender experiments substantiated the feasibility of scaleup for continuous flow operations.

OAK RIDGE NATIONAL LABORATORY
CENTRAL RESEARCH LIBRARY
DOCUMENT COLLECTION
LIBRARY LOAN COPY
DO NOT TRANSFER TO ANOTHER PERSON
If you wish someone else to see this document, send in name with document and the library will arrange a loan.
UCN-7969
(3 3-67)

Oak Ridge Station
School of Chemical Engineering Practice
Massachusetts Institute of Technology

[redacted]

Removed
Per LRD
3/25/77
bcr

CONTENTS

Page

1. Summary 4
2. Introduction 4
3. Apparatus and Procedure 5
   3.1 Systems Investigated 5
   3.2 Apparatus 6
   3.3 Experimental Procedure 6
      3.3.1 Flow Studies 6
      3.3.2 Blender Experiments 9
4. Results 10
   4.1 Bubble Size Distribution 10
   4.2 Gas Loading 13
   4.3 Blender Experiments 17
5. Discussion of Results 17
   5.1 Gas Loading Mechanism 17
   5.2 Bubble Size Distribution 20
   5.3 Blender Experiments 21
6. Conclusions 22
7. Recommendations 22
8. Acknowledgements 23
9. Appendix 24
   9.1 Average Diameter with Chopping Mode of Dispersion 24
   9.2 Sampling Procedure 25
   9.3 Location of Original Data 25
   9.4 Nomenclature 25
   9.5 Bibliography 26

1. SUMMARY

An investigation of the parameters affecting gas dispersion in highly viscous liquids was conducted. The practical application of this study would be in the dispersion of radioactive krypton and xenon in molten glass for long-term waste disposal. Argon and polybutene were used to simulate this system. The parameters studied were gas flow rate, impeller speed, impeller geometry and position of gas inlet relative to direction of liquid flow. An experimental gas dispersion apparatus was used to study these parameters in a flow system. It was found that the impeller blade pitch had little effect on gas loading at high rpm's, but that at low rpm's average bubble size decreased slightly with increased impeller blade pitch. Volumetric percent gas loading increased linearly with impeller speed. The rate of increase in loading with rpm appeared to increase with gas flow rate. The maximum loading obtained in the flow system was 12.6% at a gas feed rate of 14.5 sccm, a liquid flow rate of 95 cc/min, and an impeller speed of 1740 rpm.

Blender experiments were conducted to study maximum gas loading obtainable in polybutene at ambient temperature and pressure. A maximum of 24.8% was found. A blender flow experiment, yielding 20% loading, indicated the feasibility of scaleup for a continuous flow operation.

It is recommended that further studies be made using a modified mixing chamber in the present apparatus. Blender-type experiments should also be conducted to study the effect of liquid viscosity on the dispersion of gas and to determine scaleup parameters. Residence time in the mixing region, temperature profile, and power input should be determined in future studies. Optimum gas flow rate and optimum impeller speed must also be determined.

2. INTRODUCTION

As nuclear power plants become more numerous, the associated problem of radioactive waste disposal is becoming more acute. Containers for such waste materials must be resistant to high temperatures and possible chemical degradation resulting from the intense radiation. In addition, materials of construction must be such as to remain intact over long periods of time, resisting attack by both the waste and the environment. The radioactive isotopes of the noble gases, krypton and xenon, present a particular disposal problem. Compounds of krypton and xenon are known, but they do not have the chemical stability required for long-term storage (2).

The methods presently being used for disposal of noble fission product gases include controlled release to the atmosphere, injection underground, and storage in pressurized gas cylinders (2). More recently the possibility of storage in foamed glass has been considered as a method for containment of radioactive krypton and xenon. Glasses are chemically inert in most environments, are resistant to radiation, and have good mechanical strength properties at high temperatures. In addition, foams have an advantage over

other containers since, in the event of accidental breakage, only a small fraction of the gas bubbles will be ruptured. This fact minimizes the potential radiation contamination hazard.

To evaluate the feasibility of radioactive gas containment in glass foams, it will be necessary to investigate a technique for producing a glass foam with a high loading of small gas bubbles. However, at the high viscosities characteristic of molten glass, bubble dispersion becomes difficult, and the mechanics of the process are not well understood.

The objective of this study was to analyze experimentally the various parameters affecting the dispersion of a gas in a highly viscous liquid. The variables which were considered to be pertinent to and within the realm of this study were gas flow rate, impeller speed, impeller geometry, and gas inlet position relative to direction of flow.

3. APPARATUS AND PROCEDURE

3.1 Systems Investigated

Because of its high viscosity and Newtonian characteristics, polybutene grade 16, manufactured by the Oronite Division of Standard Oil of California, was used to simulate molten glass. Table 1 shows the more important physical properties of the polybutene used in this study. The dispersed phase in all experiments, except those involving the blender, was argon supplied from a standard pressure cylinder. In the blender studies, atmospheric air was entrained in the fluid. All studies were conducted at room temperature (80°F).

Table 1. Physical Properties of Polybutene Oronite Grade 16

Condition	clear, bright, free from sediment
Color	pale yellow
Specific gravity at 60/60°F	0.880
Average molecular weight	640
Viscosity at room temperature (80°F)	2380 centistokes (3110 cs measured)
Viscosity at 100°F	1230 centistokes
Viscosity at 210°F	53 centistokes
Flash point	335°F
Pour point	-10°F
Coefficient of thermal expansion per °C (15°C - 100°C)	0.00074

Values given are from manufacturer's brochure. Values in parentheses were measured. The reason for the difference between measured and manufacturer's values is not known.

3.2 Apparatus

The experimental gas dispersion apparatus employed in the flow studies is shown in Fig. 1. It consisted of a 55-gal feed drum for the polybutene, a mixing chamber of about 920 cc, a vertical flow chamber with a window port for photographing the dispersed bubbles, and a dual outlet-sample duct. Polybutene flow was regulated by means of a 1 in. ball valve in the feed line. The mixing chamber was fitted with a variable speed impeller mount and an 0.011 in. orifice in the bottom of the chamber through which argon was introduced. The circumferential position of the orifice with respect to the impeller could be varied. There were two view ports in the vicinity of the impeller, allowing observation of flow patterns in the mixing region. For the blender experiments, a Waring blender was employed. The top was open to allow atmospheric air to be dispersed in the polybutene.

Apparatus for a flow experiment utilizing the blender is shown in Fig. 2. Flow through the system was induced by aspirator suction. A graduated cylinder was used for sampling.

3.3 Experimental Procedure

3.3.1 Flow Studies

Experiments were conducted in two impeller speed ranges. At low rpm (200-600), steady state bubble distributions were photographed through the vertical viewing port. In the higher range (600-1740 rpm), the dispersion became too dense to be characterized photographically. Samples of the two-phase system were taken, and volumetric percent gas loading was measured. The sampling procedure employed a 100 ml centrifuge separatory funnel inserted in the outlet sampling port. The polybutene-argon mixture was allowed to flow through this sampling bottle for approximately 3 min, after which the bottle was removed from the outlet line and allowed to stand. The settled volume was noted and the percent gas calculated.

Parameters varied include gas flow rate, impeller type, and impeller speed. Three impellers were employed. All were four-bladed, 2.125 in. diameter, and otherwise identical except for the blade pitch which was set at 45°, 15°, and 0° from the horizontal. Table 2 outlines the experiments conducted in this section. (All symbols are defined in Appendix 9.4).

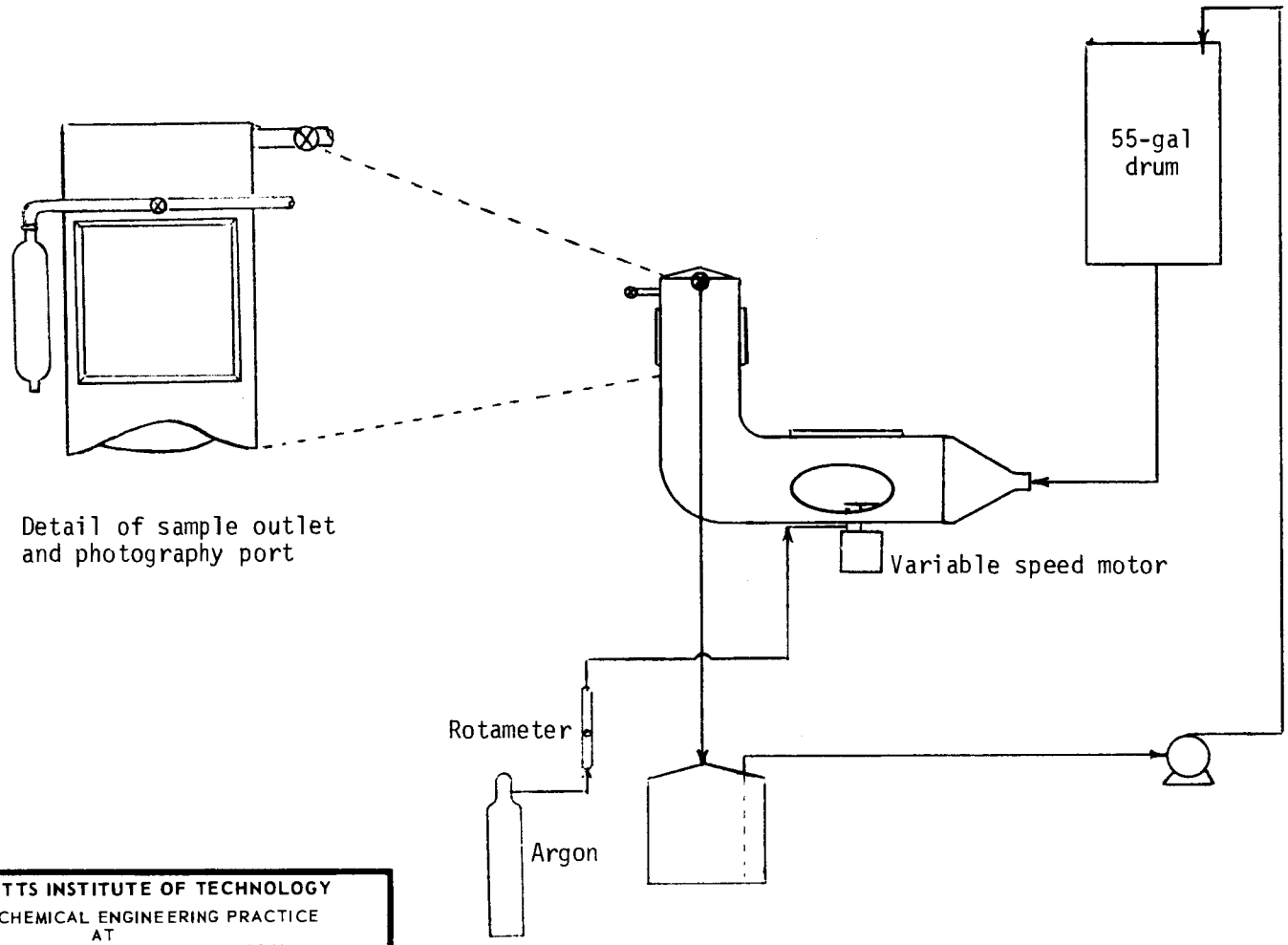

MASSACHUSETTS INSTITUTE OF TECHNOLOGY SCHOOL OF CHEMICAL ENGINEERING PRACTICE AT OAK RIDGE NATIONAL LABORATORY			
EXPERIMENTAL GAS DISPERSION APPARATUS			
DATE 5-7-69	DRAWN BY LSB	FILE NO. CEPS-X-81	FIG. 1

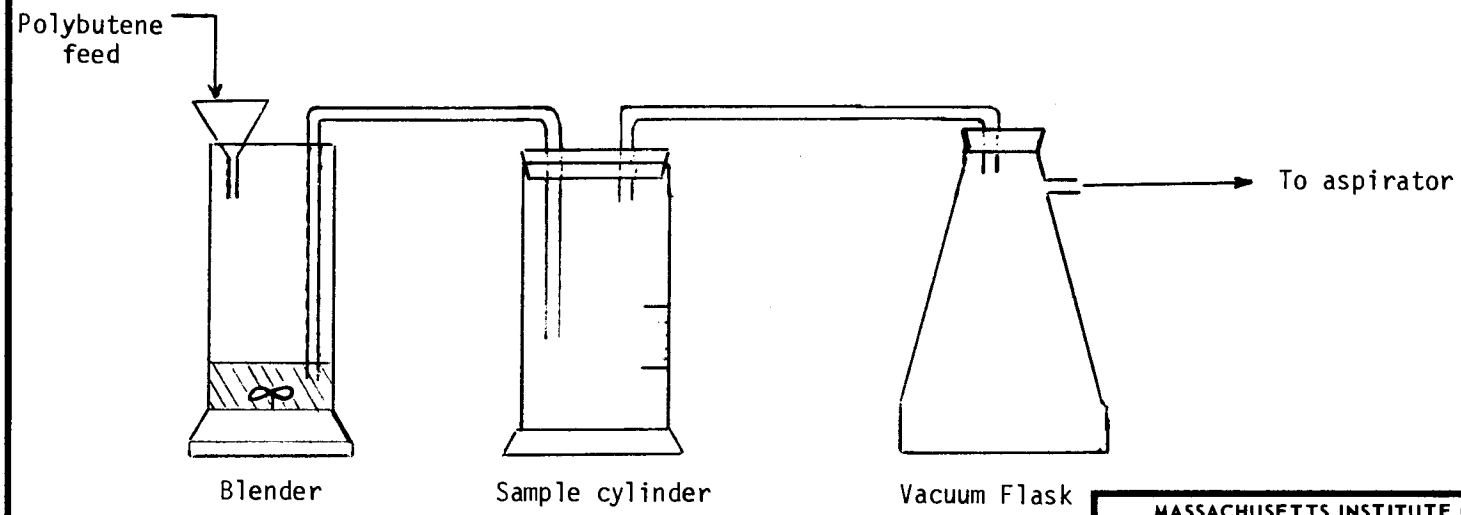

MASSACHUSETTS INSTITUTE OF TECHNOLOGY
SCHOOL OF CHEMICAL ENGINEERING PRACTICE
AT
OAK RIDGE NATIONAL LABORATORY

BLENDER FLOW APPARATUS

DATE	DRAWN BY	FILE NO.	FIG.
5-7-69	LSB	CEPS-X-81	2

Table 2. Experimental Runs to Study Gas Loading

Impeller Rotational Speed (rpm)	Gas Flow Rate (scc/min)		
	9.5	12.5	14.5
600	1, 2		1
800	1, 2, 3	2	1, 2
1000	1, 2, 3	1, 2	1, 2
1200	1, 2, 3	2	1, 2
1400	1, 2, 3	1, 2	1, 2
1600	1, 2, 3		2
1740			1

Impeller type: 1 = 45°, 2 = 15°, and 3 = 0°.

Preliminary studies were conducted to determine the optimum placement of the orifice. Photographs were taken of the dispersions resulting from the introduction of gas at the various locations. As a result of this investigation, the orifice was positioned on the side of the impeller opposite the direction of polybutene flow for all studies in this apparatus.

3.3.2 Blender Experiments

Batch experiments were conducted to study the maximum gas loading of polybutene. A volume of 200 ml of polybutene was agitated at low speed (~12,000 rpm) in the blender for varying periods of time from 30 sec to 6 min. One check experiment was made at high speed (~17,000 rpm) to ascertain whether maximum loading had been attained. Gas loading was measured by pouring the foamed polybutene into graduated cylinders. The initial and final volumes were noted and percent loading calculated.

A flow experiment was performed to investigate the feasibility of scaleup. Prior to starting flow, 200 ml of polybutene was agitated in the blender at low speed for 3 min. After flow had been started by pulling a vacuum on the sample cylinder, fresh polybutene was fed to the blender from a funnel. There was no accurate control of the polybutene feed rate or of the sample withdrawal rate. The sample cylinder was removed when it appeared that steady state had been attained.

4. RESULTS

4.1 Bubble Size Distribution

An attempt was made to characterize the size distribution of bubbles found in the flow apparatus at low rpm. Figure 3, a representative curve (at 200 rpm, with a 45° impeller, and a gas flow rate of 9.5 sccm), is fairly characteristic of bubble size distributions obtained throughout the study. All distributions showed a preponderance of small bubbles (0.1 - 0.2 mm), the number dropping off rapidly between 0.3 and 0.4 mm. Approximately 500 bubbles were visually sized to determined average bubble size. The first method used for calculating average bubble diameter was a number mean, where

$$d_{av} \equiv \frac{\sum_i n_i d_i}{n_{total}}$$

Only insignificant variations in average size could be found, with average bubble diameter being approximately 0.3 mm when rounded off to the accuracy of visual sizing (see Table 3). A second method was used to weight the larger, more easily observed bubbles more heavily. This was a volume-to-surface mean diameter (Sauter method) where

$$d_{32} \equiv \frac{\Sigma n_i d_i^3}{\Sigma n_i d_i^2}$$

Again, no simply characterized trend was apparent from the limited data. The percentage of bubbles greater than 0.5 mm (the size considered as a large bubble) was calculated from the bubble counts using the following equation:

$$\% \text{ of bubbles} > 0.5 \text{ mm} \equiv \frac{\sum_{d>0.5 \text{ mm}} n_d}{n_{total}}(100)$$

In these low rpm experiments, only a small fraction of the gas pumped into the system was dispersed as small bubbles. The bulk of the gas left the system as very large bubbles. These large bubbles were not characterized or included in any of the average diameter calculations above. A compilation of the results of the low rpm flow studies may be found in Table 3.

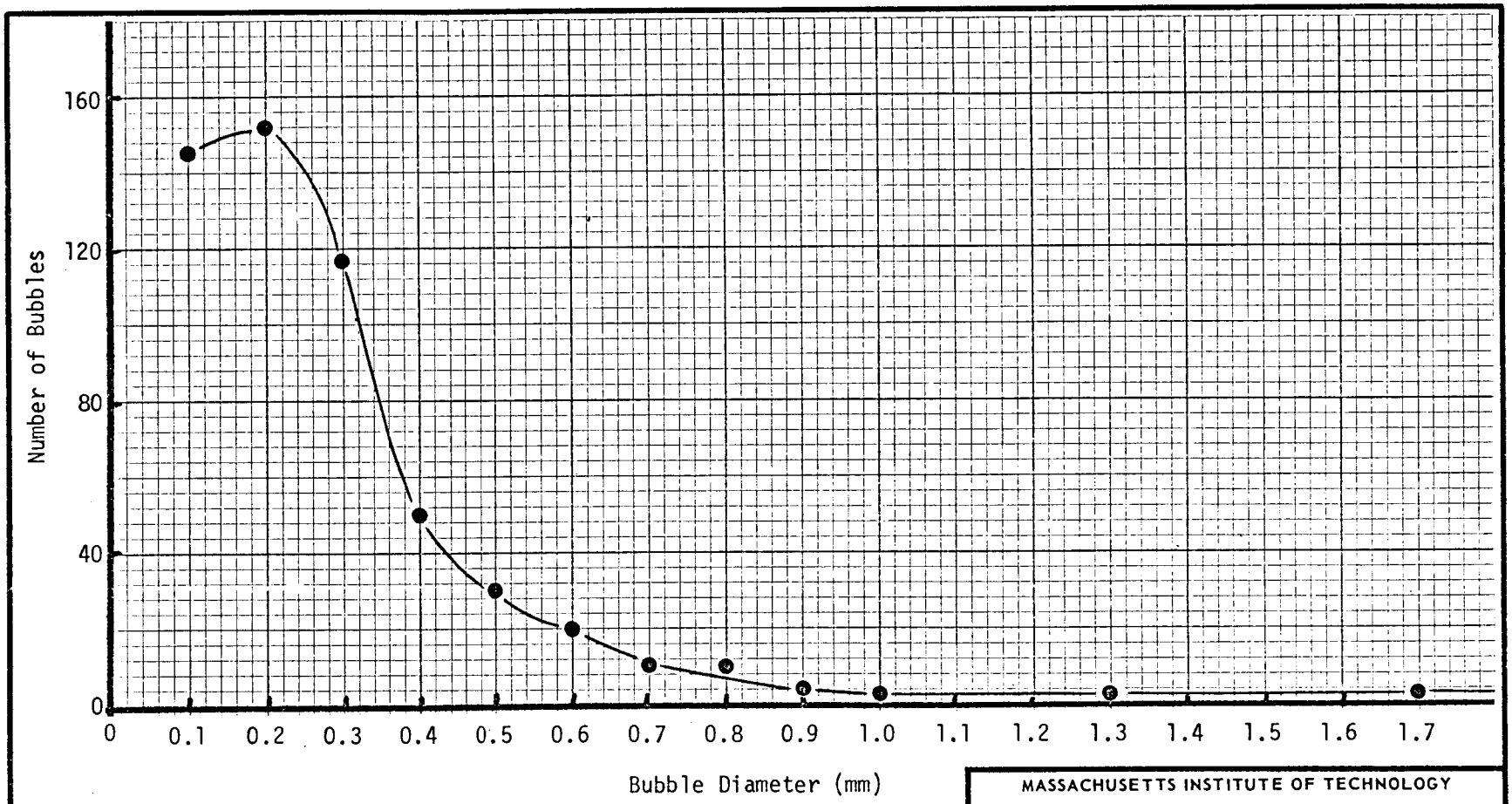

MASSACHUSETTS INSTITUTE OF TECHNOLOGY
SCHOOL OF CHEMICAL ENGINEERING PRACTICE
AT
OAK RIDGE NATIONAL LABORATORY

BUBBLE SIZE DISTRIBUTION
(45° impeller, 200 rpm, 9.5 sccm gas flow rate)

DATE	DRAWN BY	FILE NO.	FIG.
5-7-69	MHJ	CEPS-X-81	3

Table 3. Results of Bubble Size Distribution

Rotational Impeller Speed (rpm)	d_{av} (mm)	d_{32} (mm)	% of bubbles > 0.5 mm[1]
Gas flow rate = 9.5 sccm, 45° impeller			
200	0.29	0.87	9.4
300	0.29	0.62	10.8
400	0.30	0.78	10.3
500	0.26	0.45	4.9
Gas flow rate = 14.5 sccm, 45° impeller			
200	0.29	1.25	5.1
300	0.34	0.49	6.2
400	0.27	0.61	7.2
500	0.24	0.47	2.7
Gas flow rate = 9.5 sccm, 15° impeller			
200	0.36	1.27	7.1
300	0.38	1.91	11.4
400	0.36	1.23	15.5
500	0.29	0.90	7.3

[1]This percent does not include the very large bubbles which escaped from the system uncounted. The greatest fraction of the volume of gas pumped into the system escaped as very large bubbles which were not characterized or counted.

4.2 Gas Loading

A summary of gas loading results is shown in Table 4. In the impeller speed ranges studied in this section, gas-filled vortices formed around the impeller. Periodically, gas from these vortices would overflow into the vertical section of the apparatus as large bubbles (2-5 mm in diameter). These large volumes of gas escaped from the sample bottles before the initial volume of the foam could be measured. Therefore, the volume percentages of argon in Table 4 are an indication of the amount of gas which was entrained in the viscous fluid as small bubbles. The maximum loading is defined as that loading which would be obtained if all of the gas put into the system were dispersed as small bubbles in the polybutene at given gas and liquid flow rates.

Gas loading results obtained at various impeller speeds for a fixed impeller geometry are shown as the percent of maximum loading in Fig. 4. Impeller speeds ranged from 600 rpm to 1740 rpm, the highest possible with the motor used. As shown, the gas loading increased linearly with impeller speed. Three gas flow rates are presented in this figure: 14.5, 12.5, and 9.5 sccm, the slopes of the lines being 0.82, 0.54, and 0.21, respectively. The highest gas loading obtained in this apparatus was 95.5% of maximum, employing a gas flow rate of 14.5 sccm and an impeller speed of 1740 rpm.

The effect of impeller geometry on gas loading (using a fixed gas flow rate) over an impeller speed range of 600 rpm to 1600 rpm is shown in Fig. 5. There is significant difference for the different pitches, but too much scatter to justify separate curves. It is interesting to note that slightly higher gas loadings were obtained with the 0° blade-pitch impeller than with the other blades.

Window ports at the top and side of the apparatus permitted the observation of flow patterns within the mixing chamber. The following points were observed:

1. At low speeds (200-300 rpm) the impeller dragged the bubbles away from the gas feed orifice into a spiral. Bubbles of approximately 2 mm in diameter were detached from the orifice in this manner. Shear forces in the fluid surrounding the impeller distorted these bubbles into a crescent shape.

2. Bubbles on the periphery of the mixing area were pulled in toward the center and were swept into the impeller blades.

3. At all speeds studied, there was a considerable volume of the chamber in which mixing did not occur. Polybutene from the reservoir merely flowed through these areas with little or no agitation from the impeller.

4. At the initiation of mixing, a small gas pocket would form over the center of the impeller. This gas pocket would remain relatively

Table 4. Results from Gas Loading Experiments

N (rpm)	Volume % Argon	% of Maximum
Impeller Type: 45°, G = 14.5 sccm, L = 95 ml/min, maximum G/G+L = 13.2%		
600	0.49	3.7
800	2.2	16.7
1000	2.9	22.0
1200	6.35	48.0
1400	9.0	68.0
1740	12.6	95.5
G = 12.5 sccm, L = 95 ml/min, maximum G/G+L = 11.6%		
1000	1.51	13.9
1400	3.82	32.9
1600	5.35	46.0
G = 9.5 sccm, L = 95 ml/min, maximum G/G+L = 9.1%		
600	1.99	22.0
800	1.26	13.9
1000	2.34	25.7
1200	2.16	23.7
1400	2.95	32.4
Impeller Type: 15°, G = 12.5 sccm, L = 95 ml/min, maximum G/G+L = 11.6%		
800	3.2	27.6
1200	4.0	34.5
1400	5.4	47.0
G = 9.5 sccm, L = 95 ml/min, maximum G/G+L = 9.1%		
600	1.8	19.3
800	2.3	25.1
1000	2.5	27.8
1200	3.6	39.5
Impeller Type: 0°, G = 9.5 sccm, L = 95 ml/min, maximum G/G+L = 9.1%		
800	2.3	25.1
1000	3.5	38.4
1200	4.2	46.0
1400	3.25	35.8

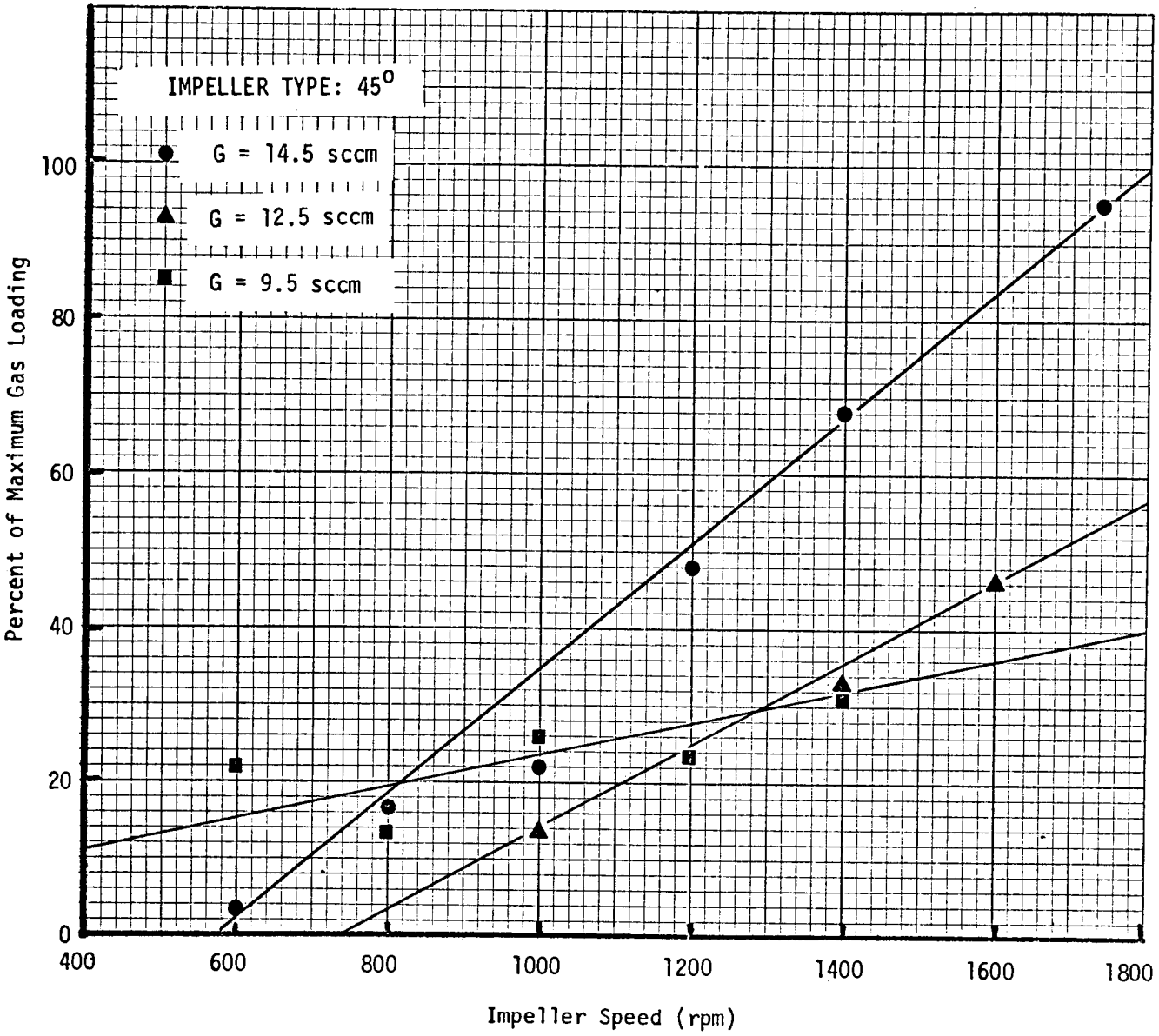

MASSACHUSETTS INSTITUTE OF TECHNOLOGY SCHOOL OF CHEMICAL ENGINEERING PRACTICE AT OAK RIDGE NATIONAL LABORATORY			
GAS LOADING (Three Gas Flow Rates)			
DATE 5-7-69	DRAWN BY MHJ	FILE NO. CEPS-X-81	FIG. 4

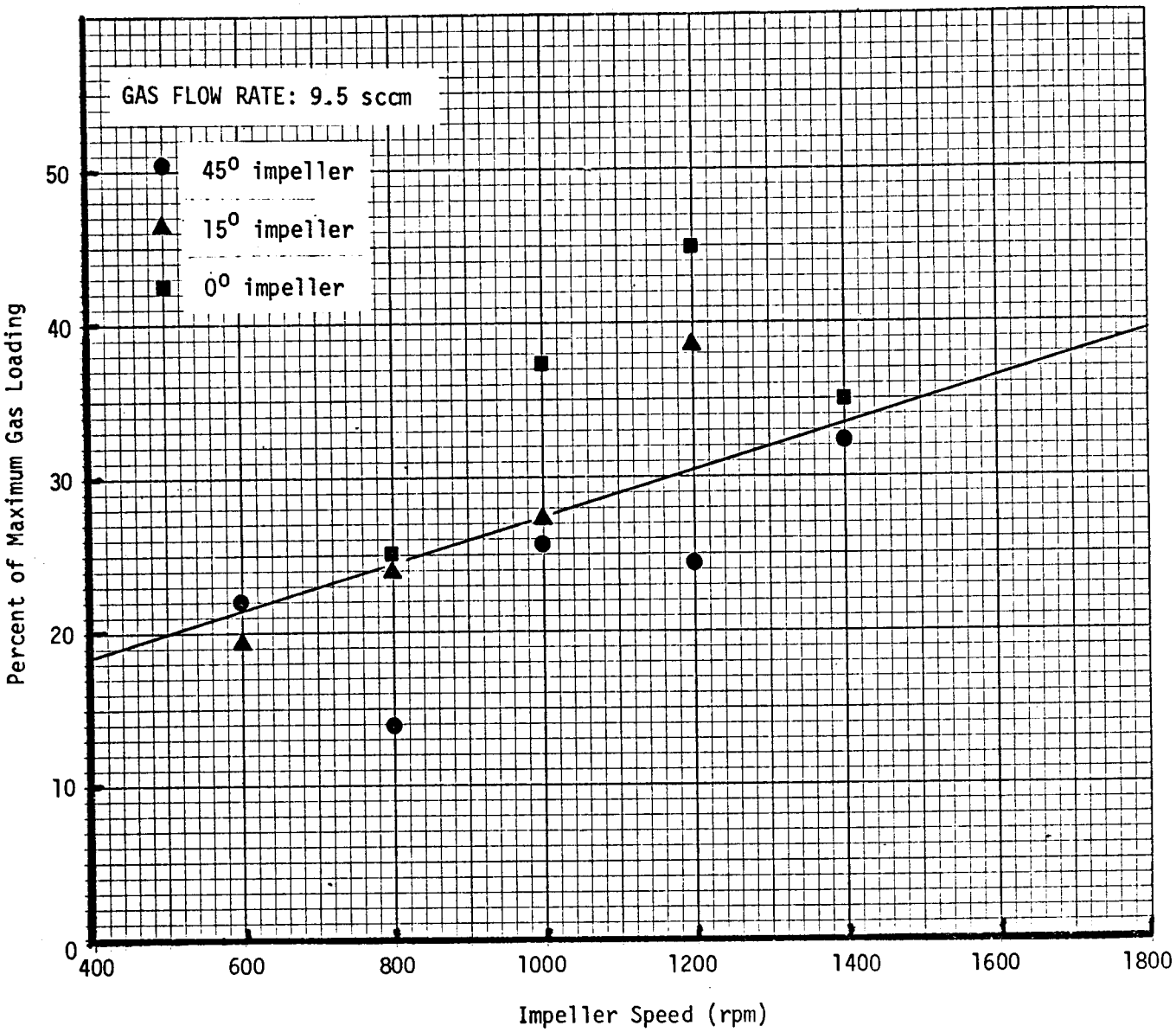

MASSACHUSETTS INSTITUTE OF TECHNOLOGY SCHOOL OF CHEMICAL ENGINEERING PRACTICE AT OAK RIDGE NATIONAL LABORATORY			
GAS LOADING (Three Impeller Geometries)			
DATE 5-7-69	DRAWN BY MHJ	FILE NO. CEPS-X-81	FIG. 5

constant in size for a period of from 10-15 min, after which it would increase in volume. Vortexing of the liquid below this gas pocket occurred after a short time, depending on the gas flow rate and impeller speed. Occasionally large bubbles from this gas void would flow into the vertical section of the apparatus.

5. Distinct bubble swirls were observed above and below the impeller and around the orifice.

4.3 Blender Experiments

With batch mixing at the lower blender speed (∿12,000 rpm), the time required to obtain the highest gas loading of air in polybutene is shown in Fig. 6. Up to a stir time of 3 min, there was an increase in percent loading with time. The highest gas loading of 24.8% was attained at a stir time of 3 min. At a longer stir time of 6 min, a slight decrease in gas loading (to 23.2%) was found. During this time the temperture of the polybutene had increased by 22.5°C due to heat generation in the blender. This temperature increase would correspond to a viscosity decrease in the pure polybutene of 18.3 poise. A similar decrease in gas loading (to 22.1%) was found when the blender was run at high speed (∿17,000 rpm) for 3 min; the temperature increase was 23.5°C (corresponding to a viscosity decrease of of 18.7 poise for pure polybutene). In the flow experiment, a gas loading of 20% was obtained.

The foams which were obtained using the blender were opaque and contained no bubbles of diameter greater than 1 mm. It was observed that the best foams were obtained when the level of polybutene was just above the blender impeller.

5. DISCUSSION OF RESULTS

5.1 Gas Loading Mechanism

Several experimental observations were made which are significant in aiding our understanding of the mechanism of gas dispersion and in helping us plan future experiments. First, at low impeller speeds (200-500 rpm), the 45° impeller generated bubbles with a mean diameter 75% that of the bubbles generated with the 15° impeller under the same conditions. (This is discussed further in Sect. 5.2.) Second, the curves of percent of maximum loading vs impeller speed (Fig. 4) obtained at high impeller speed (600-1600 rpm) were linear for a given impeller at a given gas flow rate. Third, these curves had higher slopes at higher gas flow rates. Fourth, the scatter in the data of percent maximum loading vs impeller speed (Fig. 5) was too great to draw any quantitative conclusions; however, the impellers with the lower blade angles appeared to give higher percent maximum loadings.

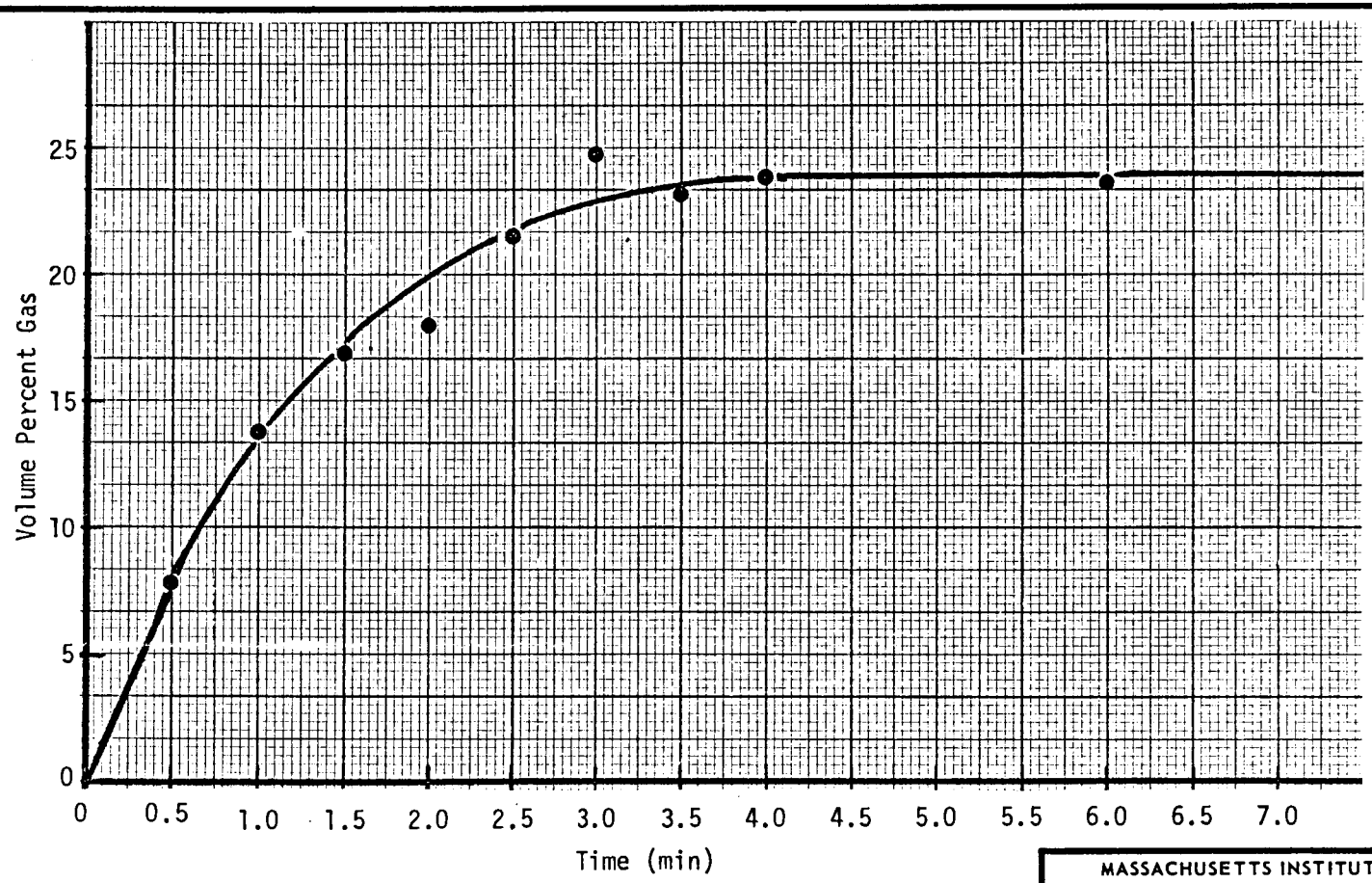

MASSACHUSETTS INSTITUTE OF TECHNOLOGY
SCHOOL OF CHEMICAL ENGINEERING PRACTICE
AT
OAK RIDGE NATIONAL LABORATORY

GAS LOADING IN BLENDER

DATE	DRAWN BY	FILE NO.	FIG.
5-7-69	MHJ	CEPS-X-81	6

The first point can be explained if it is assumed that, at low impeller speeds, the liquid surface is unaffected by the motion of the impeller. Consider the two diagrams shown below.

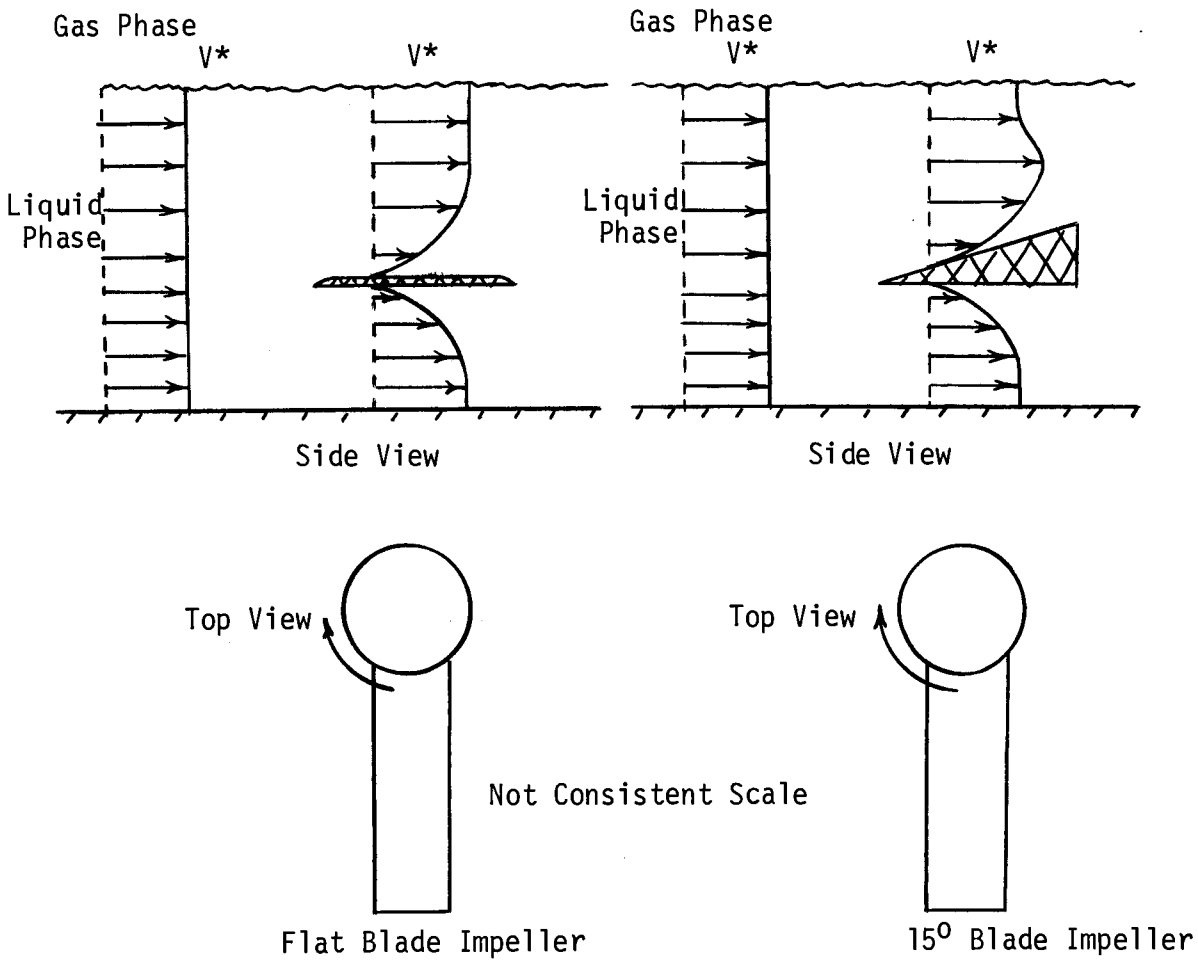

*V = rotational velocity of liquid relative to blade at radius r.

For the flat impeller, the velocity is a smooth function increasing in the direction normal to the blade surface, whereas for the 15° impeller, the continuity equation dictates that there must be a peak in the velocity profile near the solid impeller surface which is not parallel to the local direction of blade motion.

It is possible that the dispersion of bubbles can be attributed to the deformation and eventual breakup of the large bubbles that flow into a region of non-uniform velocity. It is quite likely that a 15° impeller blade would produce larger velocity gradients than would a flat blade, and that a 45° impeller blade would produce larger velocity gradients than would a 15° blade at the same speed. Therefore at low impeller speed, one would expect smaller bubbles to be produced with a 45° impeller than with a 15° impeller. The phenomena that would occur at higher impeller speeds, where the liquid surface is disturbed by the motion of the impeller, are expected to be more complex.

The second observation, that the percent maximum loading vs impeller speed curves (Fig. 4) are linear, can be explained if it is assumed that fluid motion in the vicinity of the impeller (at high speed) can be characterized by an average shear rate which is linearly related to the rotational speed of the impeller (11):

$$\left.\frac{dV^*}{dr}\right)_{avg} = k\,N$$

In this case, an increase in impeller speed (N) should cause an increase in the average shear rate, and (assuming constant viscosity) the shear stress. These changes should cause more of the large bubbles to be dispersed rather than allowing them to escape, and thus they should cause an increase in the percent maximum loading. This increase might be expected to be linear with N since the shear rate increases linearly with N.

The third observation, that the curves of percent maximum gas loading vs impeller speed had higher slopes at higher gas flow rates, cannot easily be explained. Future studies should investigate this observation by considering the effects of bubble loading on fluid viscosity and input power at a given blade speed for a given impeller. The fourth observation, that no clear distinction can be made between the impellers based on percent maximum loading vs impeller speed curves, should be verified because of the large scatter in the data. In such studies careful note should be made of power input dependence on blade geometry.

5.2 Bubble Size Distribution

Visual observations through the view port indicated that the bubble size decreased with increased impeller speed over the range studied (200-500 rpm). However, when bubble size distributions were plotted, no significant differences could be found for the various impeller speeds. This probably resulted from the limited accuracy of visually counting and sizing of bubbles pictured in fairly low resolution photographs. No functional relationship between average bubble diameter and impeller speed could be determined using either the number mean diameter (d_{av}) or the volume-to-surface mean diameter (d_{32}).

Impeller geometry appeared to have a slight effect on bubble size at the low rpm's studied. At a given impeller speed, the 45° impeller generated smaller bubbles than did the 15° impeller; i.e., the average (number-mean) diameter of the bubbles generated by the 45° impeller was approximately 75% of that generated by the 15° impeller. This result suggests that argon was dispersed into the polybutene by viscous shear forces rather than by a purely physical mechanism of chopping bubbles from the orifice. If a chopping mechanism with no further breakup of the bubbles by viscous shear were dominant, the diameter of the bubbles would have been approximately three times larger than those observed (see

Appendix 9.1). Also, impeller blade pitch should have had no effect on the size of bubbles at a given impeller speed if the blade served only to chop the bubble from the orifice. The dispersion mechanism is discussed in more detail in Sect. 5.1.

At the low speeds studied, the diameter of the bubbles did not appear to be a function of gas flow rate. Any effect which it has is probably masked by incomplete mixing in the mixing chamber. Gas loading was not thoroughly studied at the low impeller speeds for which size distribution was measured because not enough gas was entrained in a 100 ml sample to accurately measure it. However, the few samples taken indicated that gas loading is also independent of gas flow rate at low rpm's. Again, this probably results from incomplete mixing.

It is important to note that in all cases studied, mean bubble diameter was less than 0.5 mm. It has been suggested (2) that glass foams comprised of gas bubbles of diameters smaller than 1.0 mm would be acceptable for the purpose of krypton and xenon disposal. From bubble size considerations, it appears that a stirred tank flow system is a feasible means of foaming glass.

5.3 Blender Experiments

The principle upon which the blender experiments were based was that an impeller operating near the surface of a liquid will act as a self-entrainer of the gas above the surface. The mechanism of gas dispersion in polybutene in the blender is quite simple. The blender agitates the polybutene and large pockets of air are folded into it by the motion of the impeller. These large pockets of air are then broken down by the viscous shear effects in the agitated polybutene. This process is repeated over and over with a resulting well-dispersed phase of small gas bubbles. When the blending is stopped, the large air pockets break through the surface of the foam and only the very small entrapped bubbles remain dispersed.

The decrease in gas loading obtained when the blender was run for 6 min rather than 3 min at low speed and when it was operated at high speed was due to the fluid temperature increase. The calculated viscosity for pure polybutene decreases from 24.2 stokes at room temperature (27°C) to 5.94 stokes and 5.50 stokes, respectively, for the temperature increases of 22.5^{o}C and 23.5^{o}C reported in Sect. 4.3. This decrease in the viscosity allowed the entrained gas to rise very rapidly, resulting in a lower gas loading.

The flow experiment indicated that it is possible to obtain high gas loadings in a continuous flow operation. The lowest blender speed (approximately 12,000 rpm) is not indicative of the minimum rpm level necessary to attain maximum gas loading in polybutene. Since 12.6% loading was obtained in the gas flow system discussed in Sect. 4.3, it is possible that at a gas flow rate greater than the 14.5 sccm used, a 25% gas loading could be obtained at rpm's less than 5000.

6. CONCLUSIONS

1. Volume percent of gas entrained as small bubbles in an agitated highly viscous fluid increases linearly with impeller speed.

2. The rate of increase of gas loading with impeller speed increases with gas flow rate into the system.

3. No effect of impeller pitch on the gas loadings obtained at high speeds was noticed.

4. At lower speeds (rpm < 600) smaller bubbles were formed with impellers having greater blade pitches.

5. A flow system can be used for dispersing gas in highly viscous fluids. Up to 20 volume % gas loading was obtained in a flow system.

7. RECOMMENDATIONS

The mixing region of the present apparatus must be modified to achieve complete dispersion of the gas uniformly in polybutene. This could be done by: (1) baffling the present mixing chamber on the sides and bottom to channel the flow of polybutene into the vicinity of the impeller, or (2) constructing a new mixing chamber to simulate mixing similar to that in a blender. If a new mixing chamber is not constructed, it is recommended that blender flow experiments be performed to further investigate the feasibility of scaleup design for a continuous flow operation. To study shear rates lower than those attainable with the Waring Blender, a top-mounted impeller could be used. With a top-mounted impeller, the polybutene would be isolated from most of the heat generated by the motor at high speeds. Blender-type experiments would be advantageous because no gas feed system is needed, and it is easy to vary the grade of polybutene to investigate viscosity effects on gas dispersion.

If baffles are put in the present system, the following changes are recommended:

1. Introduction of argon should be from the top of the mixing chamber to prevent clogging in the gas line.

2. A good sampling procedure must be devised to facilitate gas loading determinations.

3. Impeller speeds up to 5000 rpm should be studied. The present system is limited to 1700 rpm, at which speed 100% theoretical loading at 14.5 sccm (the maximum gas rate studied) cannot be attained.

4. A pressure gauge should be installed to measure pressure of the argon over the mixing region.

6. An ammeter should be installed to study power input to the system. This would provide valuable information for defining the dispersion mechanism and for eventual scaleup design.

7. A control should be installed to accurately regulate the polybutene feed rate.

8. Thermocouples should be installed at the polybutene inlet, in the mixing chamber, at the sample port, and at the polybutene outlet to measure temperature variations in the system.

9. In future studies the effect of bubble loading on fluid viscosity should be investigated.

Values to be determined in future studies should include optimum gas flow rate, optimum impeller speed and type, and optimum residence time.

8. ACKNOWLEDGEMENTS

We would like to express our appreciation to W.E. Clark, our consultant for this investigation, to W.F. Schaffer, Jr., for his design work and help on the experimental gas dispersion apparatus, to W.N. Tillery for his guidance and assistance in photographing the results, and to D.E. Spangler for his kind assistance in providing laboratory guidance and help.

9. APPENDIX

9.1 Average Diameter with Chopping Mode of Dispersion

If mechanical chopping were the principle mode of bubble formation, then the average bubble diameter with a gas flow rate of 9.5 sccm and four bladed impeller rotating at 400 rpm would be:

$$\frac{9.5\ \text{cm}^3}{\text{min}} \times \frac{\text{min}}{400\ \text{rev}} \times \frac{\text{rev}}{4\ \text{passes}} = 0.00525\ \text{cm}^3/\text{pass}$$

$$0.00525\ \text{cm}^3 = \frac{4}{3}\pi R^3$$

$$R = \left(\frac{0.00525}{4.16}\right)^{1/3} = 0.053\ \text{cm} = 0.53\ \text{mm}$$

$$\text{average diameter of bubbles} \cong 1.06\ \text{mm}$$

To test this calculation for surface tension effects:

$$p_v - p_\ell = \frac{2\sigma}{R}$$

From Perry (3-223), σ is estimated to be 32 dynes/cm for butene.

$$p_v - p_\ell = \frac{2(32\ \text{dynes/cm})}{0.053\ \text{cm}} = 12\ \text{dynes/cm}^2$$

$$1\ \text{atm} = 1.01325 \times 10^6\ \text{dynes/cm}^2$$

$$\therefore \quad p_v - p_\ell = 0.084 \times 10^{-6}\ \text{atm}$$

The effect is negligible.

9.2 Sampling Procedure

Sampling was performed in the following manner:

1. A 100-ml centrifuge separatory funnel was attached to the sample port.

2. At the time of sampling the flow was switched to the sample port and allowed to flow through the sample bottle for approximately 3 min.

3. The flow was switched back to the outlet port; the sample bottle was removed, capped, and turned on end to allow settling out of entrained argon.

4. After the polybutene was completely clear of bubbles, a measured amount of water was pipetted into the sample until the original full sample volume was attained.

5. Volumetric gas loading was calculated by dividing the volume of water added by the volume of the sample bottle (equal to the volume of the foamed sample taken).

9.3 Location of Original Data

All laboratory data and observations are located in ORNL Notebook No. A-5577-G, pp. 1-39. This notebook together with the calculations are on file at the M.I.T. School of Chemical Engineering Practice, Bldg. 1000, ORNL.

9.4 Nomenclature

d diameter of bubble, mm

G gas flow rate, sccm (standard cubic centimeters/minute)

L liquid flow rate, ml/min

n number of bubbles

N impeller speed, rpm

p pressure

R radius of bubble, mm

V^* rotational velocity of liquid relative to impeller blade at radius r

σ surface tension, dynes/cm

9.5 Bibliography

1. Bird, R.B., W.E. Stewart, and E.N. Lightfoot, "Transport Phenomena," pp. 1-100, John Wiley & Sons, New York (1960).

2. Clark, W.E., rough draft for Chem. Tech. Div. Ann. Progr. Rept., ORNL, April 1969.

3. DeVries, A.J., "Foam Stability. Part I. Structure and Stability of Foams," Recueil, 77, 81 (1957).

4. Gottlieb, M.H., "Bubble Stability in Dimethylsilicone Solutions," The Research Laboratories, Interchemical Corp., New York (March 2, 1959).

5. Hinze, J.O., "Fundamentals of the Hydrodynamic Mechanism of Splitting in Dispersion Processes," A.I.Ch.E. Journal, 1(3), 289 (1955).

6. Manfré, G., "Rheological Aspects of Drop Formation," J. Appl. Phys., 37(5), 1955 (1966).

7. Metzner, A.B., and R.E. Otto, "Agitation of Non-Newtonian Fluids," A.I.Ch.E. Journal, 3(1), 3 (1957).

8. Myers, R.R., J.C. Miller, and A.C. Zettlemoyer, "The Splitting of Thin Liquid Films. Kinematics," J. Coll. Sci., 14, 287-299 (1959).

9. Perry, J.H., "Chemical Engineers' Handbook," 4th edition, pp. 18-81/18-82, McGraw-Hill, New York (1963).

10. Rea, H.E., Jr., and T. Vermeulen, "Effect of Baffling and Impeller Geometry on Interfacial Area in Agitated Two-Phase Liquid Systems," UCRL-2123, University of California Radiation Laboratory, Livermore (April 3, 1953).

11. Rushton, J.H., and J.Y. Oldshue, "Mixing-Present Theory and Practice," Chem. Eng. Progr., 49(4), 161 (1953).

12. Vermeulen, T., G.M. Williams, and G.E. Langlois, "Interfacial Area in Liquid-Liquid and Gas-Liquid Agitation," Chem. Eng. Progr., 51(2), 85-F (1955).

13. Wace, P.F., and D.L. Banfield, "Foam Separation," reprinted from Chem. and Proc. Eng. (October 1966).

14. Yang, Wen-Jei, and Hsu-Chieh Yeh, "Theoretical Study of Bubble Dynamics in Purely Viscous Fluids," A.I.Ch.E. Journal, 12(5), 927 (1966).

INTERNAL DISTRIBUTION

1. E.H. Acree
2. R.E. Blanco
3. J.O. Blomeke
4. R.E. Brooksbank
5. F.M. Browder
6. K.B. Brown
7-12. W.E. Clark
13. W. Davis, Jr.
14. D.E. Ferguson
15. C.L. Fitzgerald
16. A.P. Fraas
17. E.J. Frederick
18. H.W. Godbee
19. H.E. Goeller
20. P.A. Haas
21. Lewis Nelson
22. J.P. Nichols
23. W.F. Schaffer
24. W.E. Unger
25. M.E. Whatley
26. R.G. Wymer
27. Oak Ridge Engineering Practice School
28-29. Central Research Library
30. Document Reference Section
31-33. Laboratory Records
34. Laboratory Records, ORNL R.C.
35. ORNL Patent Office
36-50. M.I.T. Station Files

EXTERNAL DISTRIBUTION

51. W.G. Belter, AEC, Washington
52. Manson Benedict, MIT
53. S.M. Fleming, MIT
54. E.A. Mason, MIT
55. C.W. Selvidge, MIT
56. T.J. Thompson, MIT